Science Advances
AAAS

Supplementary Materials for

Living microecological hydrogels for wound healing

Guopu Chen *et al.*

Corresponding author: Yuanjin Zhao, yjzhao@seu.edu.cn

Sci. Adv. **9**, eadg3478 (2023)
DOI: 10.1126/sciadv.adg3478

This PDF file includes:

Figs. S1 to S18

Supplementary Figures

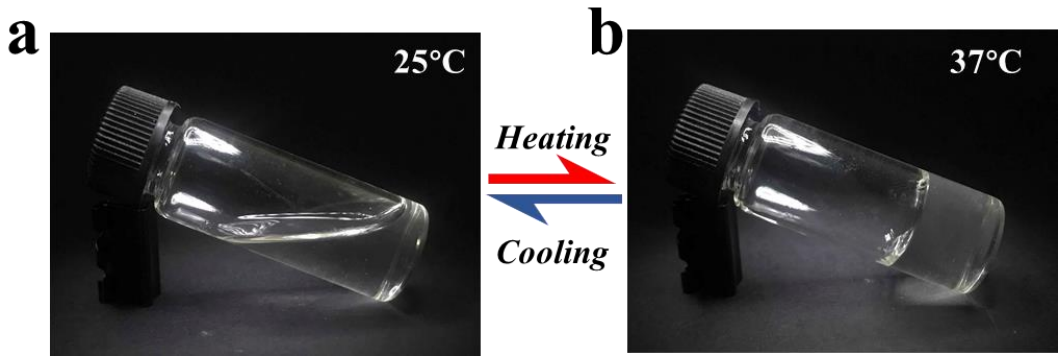

Fig. S1. **The thermosensitive gelation process of simple Pluronic F127.** The Pluronic F127 kept liquid at low temperature while quickly solidified at body temperature.

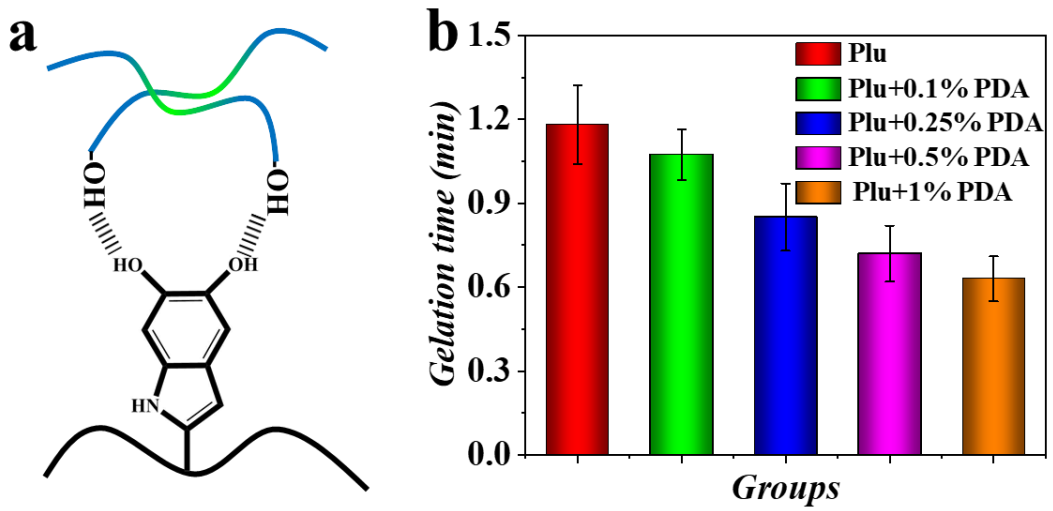

Fig. S2. The gelation time affected by the addition of PDA. (a) Hydrogen bond force may accelerate the gelation time of the hybrid hydrogel. (b) Gelation time of 18% Pluronic F127 added with different concentrations of PDA.

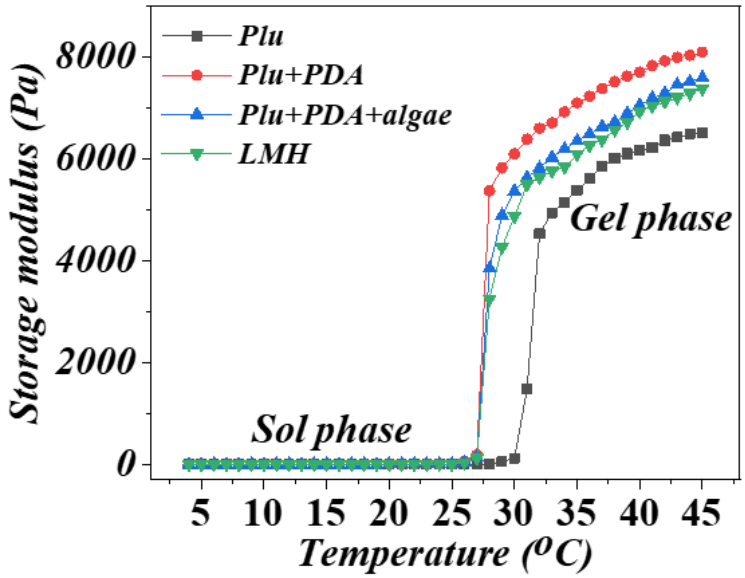

Fig. S3. Storage modulus changes of Plu, Plu+PDA, Plu+PDA+algae and LMH with temperature. Obvious sot-to-gel transition could be observed at phase-transition temperature in the four groups.

Fig. S4. The thermosensitive wet-adhesive hydrogel could write straight in the warm water. The letters M, O and C could be written in the warm water.

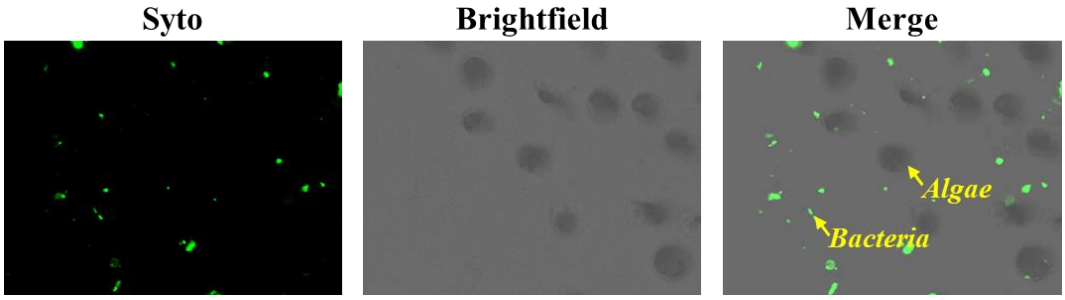

Fig. S5. Immunostaining image of the LMH. The *B. subtilis* coexisted with *Chlorella* in the hydrogel.

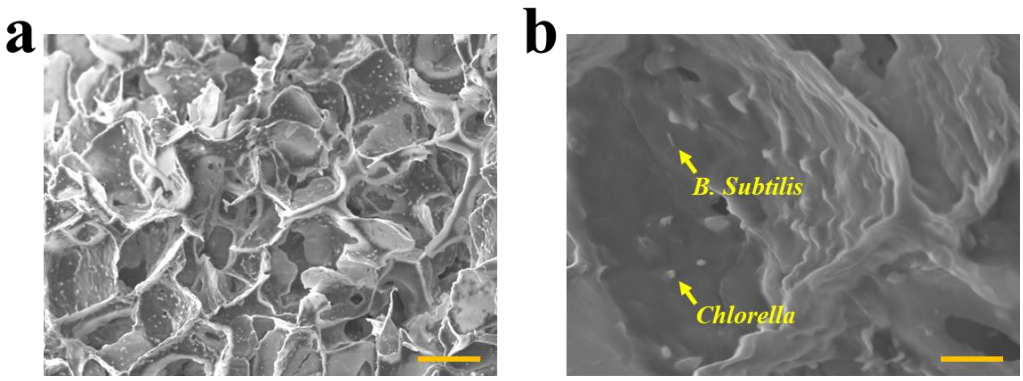

Fig. S6. Microstructure of the LMH. The (a) low-magnification and (b) high-magnification scanning electron microscope (SEM) images of the LMH. Scale bar was 50 μm in (a) and 10 μm in (b).

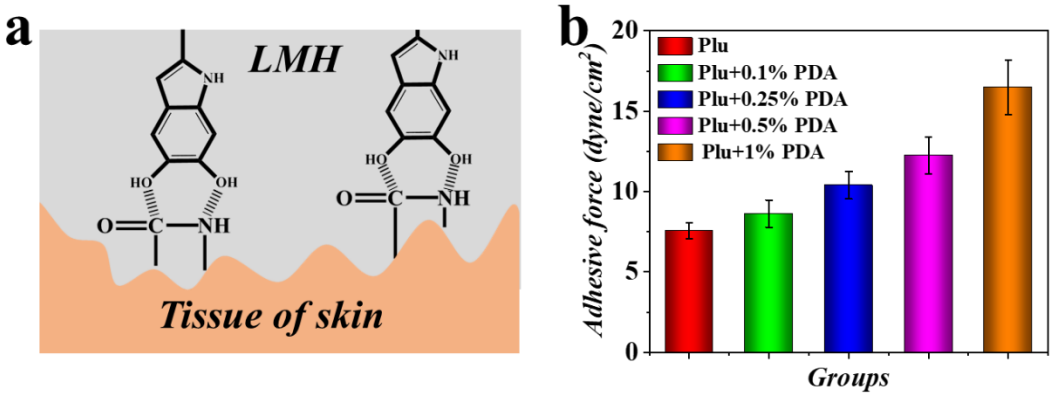

Fig. S7. The adhesive ability of the hydrogel. (a) Schematic diagram of the hydrogel adhered to the tissue surface. (b) Adhesive fore of 18% Pluronic F-127 added with different concentrations of PDA.

Fig. S8. The LMH could adhere tightly onto the human skin. Adhere at the (a) straight, (b) tilted, and (c) upside down angle.

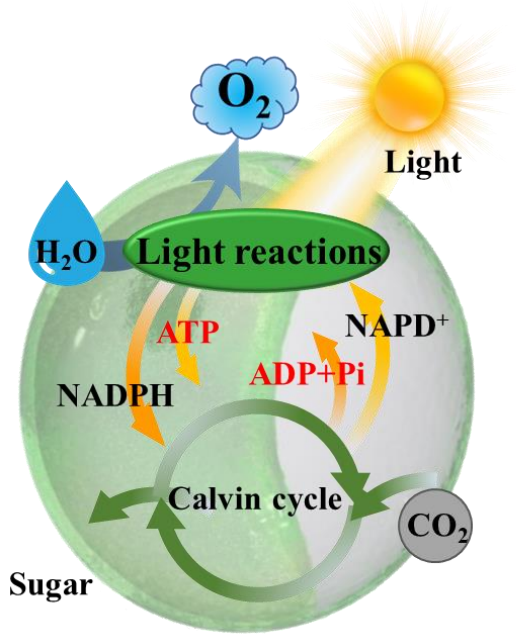

Fig. S9. Schematic illustration of light-responsive oxygen production by *Chlorella*. The algae can produce oxygen continuously under the light.

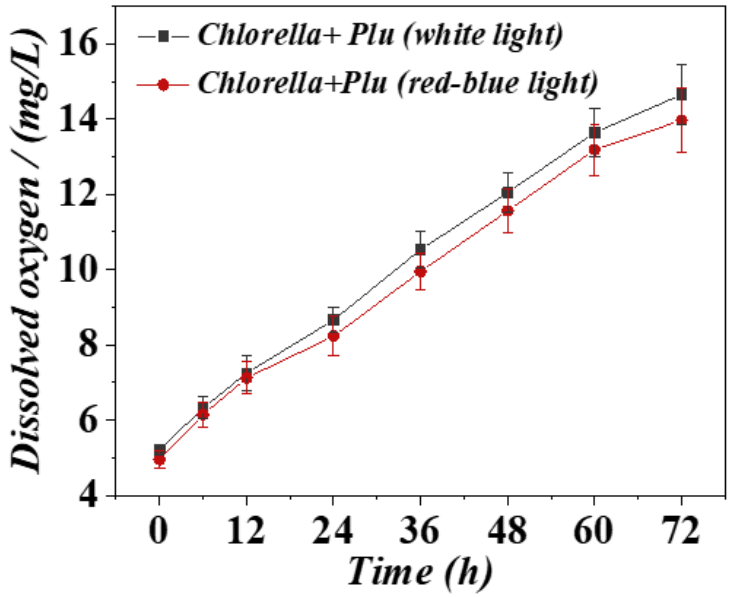

Fig. S10. The amount of dissolved oxygen released from *Chlorella* under different kinds of lights with simple Pluronic F-127 encapsulation.

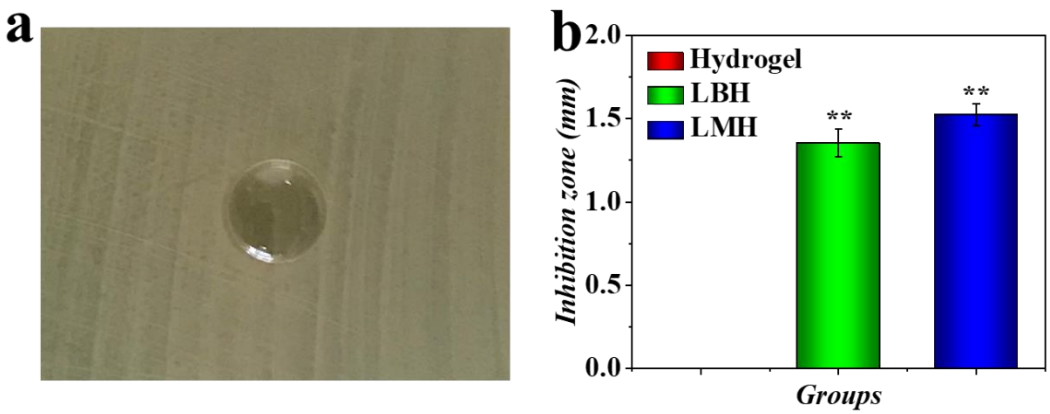

Fig. S11. Inhibition zone could be formed with the addition of *B. Subtilis*. (a) No inhibition zone could be observed in the simple hydrogel group. (b) Statistic analysis of the inhibition zone length.

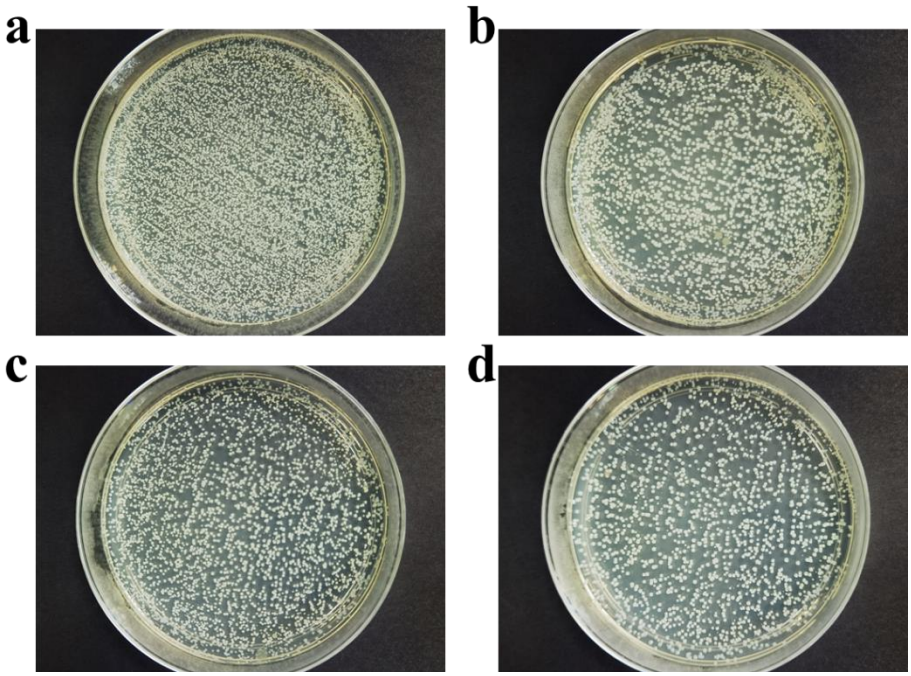

Fig. S12. Antibacterial effects of LMH against *S. aureus*. Representative images of *S. aureus*'s colony-forming units (CFUs) after co-culture with LMH at (a) 0 d, (b) 1 d, (c) 2 d, and (d) 3 d.

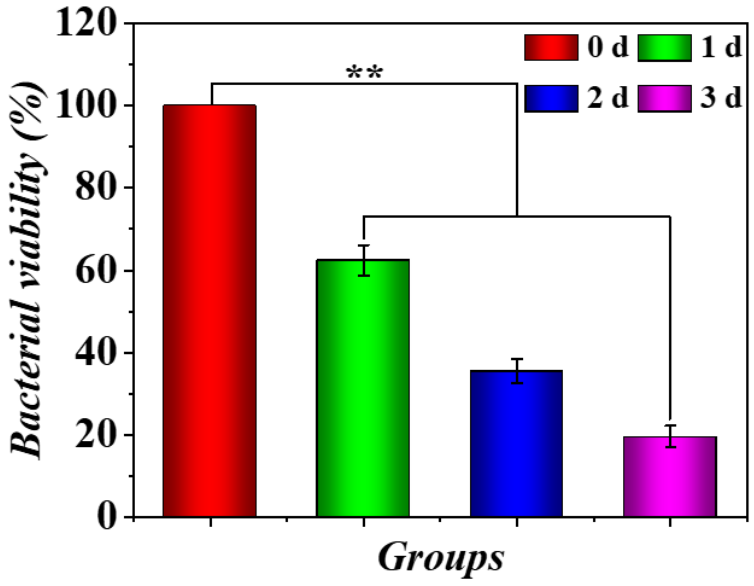

Fig. S13. Quantitative statistics of *S. aureus*'s viability after co-culture with LMH at different time points. The result of 0 d was set as 100%. The viability of *S. aureus* was observed greatly reduced due to the fengycins secreted by *B. subtilis*.

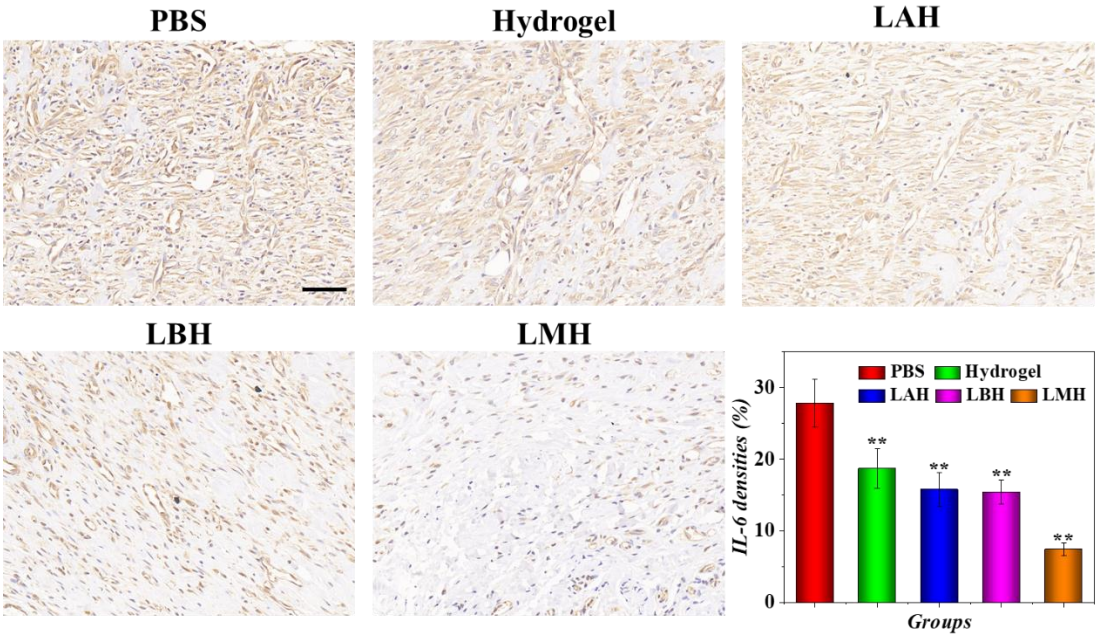

Fig. S14. Immunohistochemical staining of IL-6 in granulation tissues after 9 days. Scale bar was 100 μm.

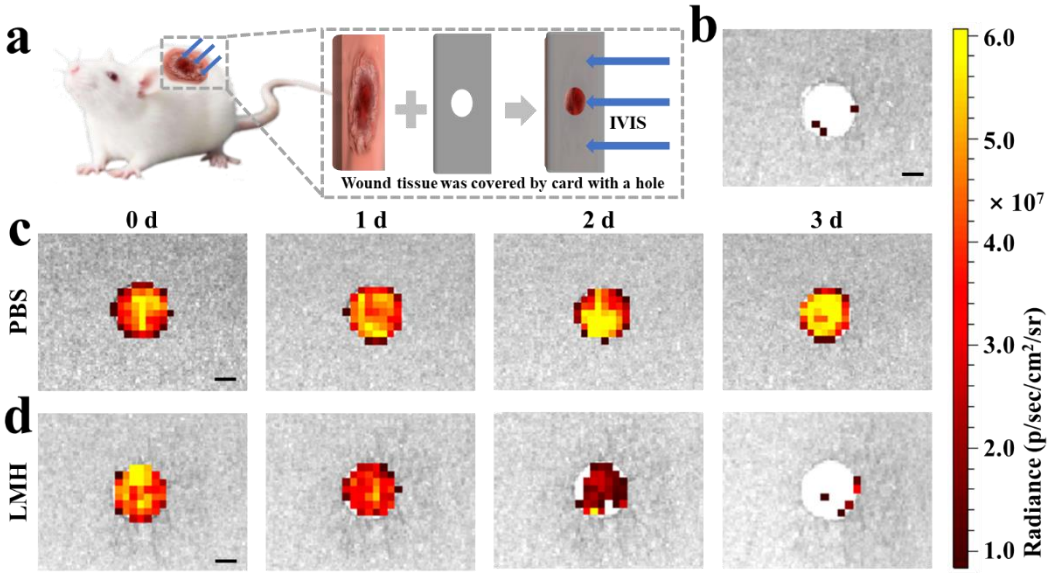

Fig. S15. The amounts of bacterial loading in the wound were evaluated by IVIS at the first three days. (a) The black card with a hole was used to cover the wound bed to eliminate fluorescent interference from hair. (b) The fluorescent image of the normal wound bed. (c) The amounts of bacterial loading in wounds treated by PBS at 0 d, 1 d, 2d, and 3d. (d) The amounts of bacterial loading in wounds treated by LMH at 0 d, 1 d, 2d, and 3d. Scale bars were 3 mm in (b-d).

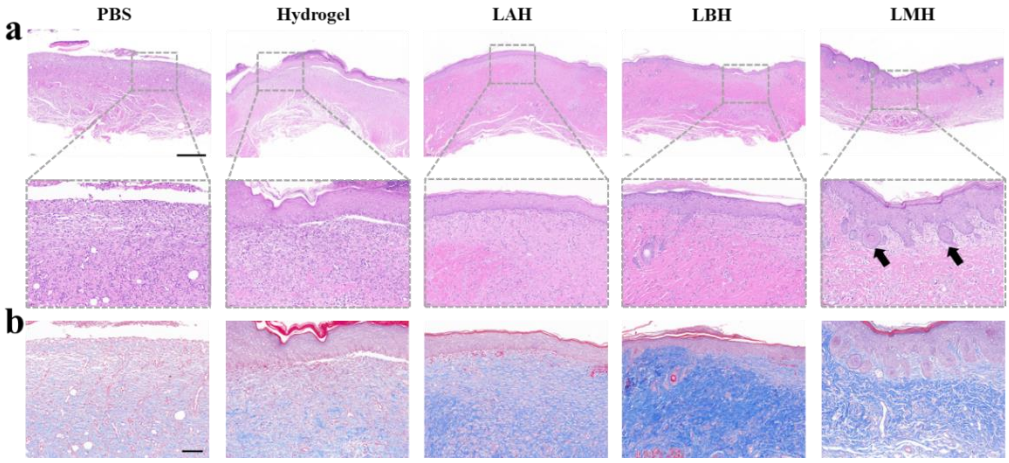

Fig. S16. The therapeutic effects of LMH on infected diabetic wounds at 12 d. (a) The regenerated granulation tissues in groups treated by PBS, Hydrogel, LAH, LBH, and LMH were stained by H&E staining after 12 d. Epithelization could be observed in Hydrogel, LAH, LBH, and LMH groups. Hair follicle regeneration could be observed in LMH group. (b) Masson trichrome staining of granulation tissues in different treatments after 12 d. Scale bar was 500 μm in (a) and 100 μm in (b).

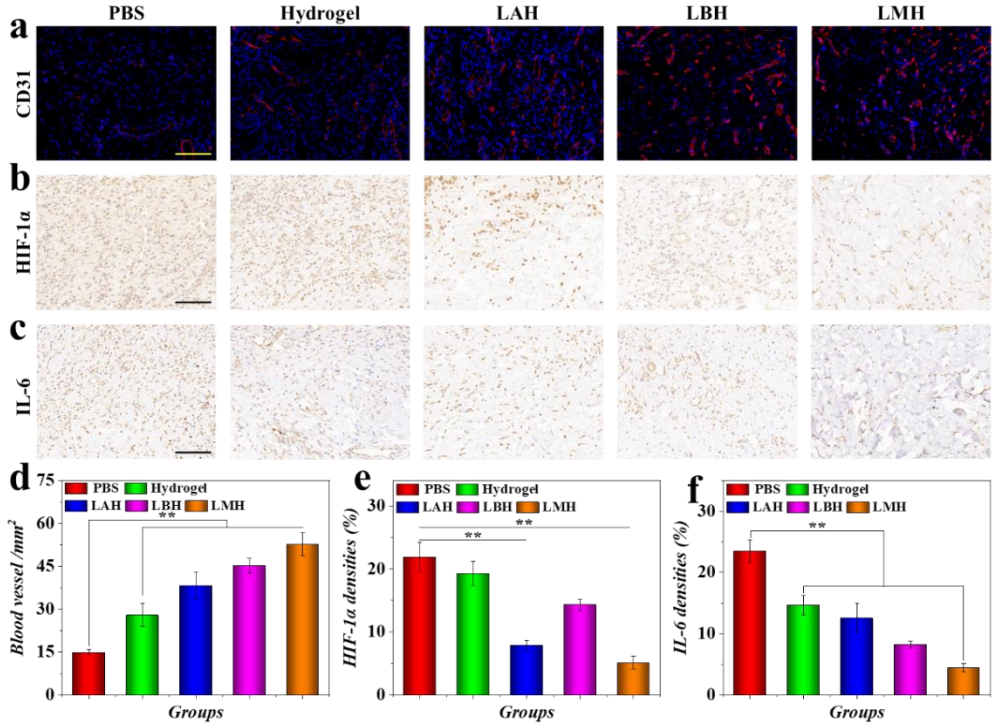

Fig. S17. The mechanism of LMH promoting chronic wound repair after 12 d. (a) The CD31-positive blood vessel endothelial cells in granulation tissues after 12 d were stained as red. (b) Immunohistochemical staining of HIF-1α in granulation tissues in different groups. (c) Immunohistochemical staining of IL-6 in granulation tissues. (d-f) Quantification of (d) blood

vessel numbers, (e) HIF-1α densities, and (f) IL-6 densities. Scale bars were 100 μm in (a-c). n=6 per group. *P < 0.05, **P < 0.01.

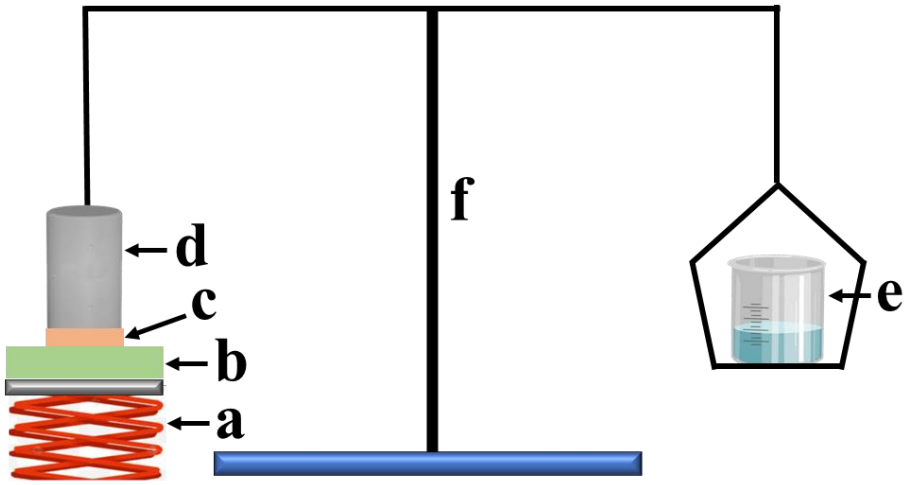

Fig. S18. Schematic illustration for detection of adhesion force. (a) Helpath Stand. (b)Hydrogel. (c)Pigskin. (d) Columella. (e)Beaker. (f) Balanced bracket.